

Two-Step Synthesis of Boron-Fused Double Helicenes

Takazumi Katayama,[†] Soichiro Nakatsuka,[†] Hiroki Hirai,[†] Nobuhiro Yasuda,[‡] Jatish Kumar,[#] Tsuyoshi Kawai,[#] and Takuji Hatakeyama^{*,†,§}

[†]Department of Chemistry, School of Science and Technology, Kwansei Gakuin University, 2-1 Gakuen, Sanda, Hyogo 669-1337, Japan

[‡]Japan Synchrotron Radiation Research Institute (JASRI)/SPRing-8, 1-1-1, Kouto, Sayo-cho, Sayo-gun, Hyogo 679-5198, Japan

[#]Graduate School of Materials Science, Nara Institute of Science and Technology (NAIST), 8916-5 Takayama, Ikoma, Nara 630-0192, Japan

[§]Elements Strategy Initiative for Catalysts and Batteries, Kyoto University, Katsura, Kyoto 615-8520, Japan

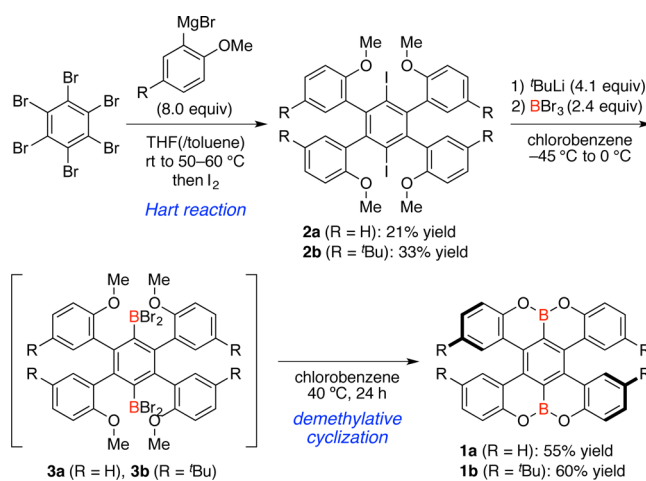
Supporting Information

ABSTRACT: Novel boron-fused double [5]helicenes were synthesized from hexabromobenzene in two steps via Hart reaction and demethylative cyclization. The parent helicene shows excellent ambipolar conductivity, which can be explained by unique 3D π -stacking with a brickwork arrangement. Moreover, the introduction of four *tert*-butyl groups suppresses racemization, enabling optical resolution. The enantiomerically pure helicene shows deep blue fluorescence with Commission Internationale de l'Eclairage coordinates of (0.15, 0.08) and circularly polarized luminescence activity.

Helicenes have attracted considerable attention because of their inherent chirality, which results in unique chiroptical properties and dynamic behavior involving self-assembly.¹ Incorporation of heteroatoms into the helicene skeleton is a promising way of changing the electronic structure and modulating physical properties.² Another approach is to introduce multihelicity, which can provide multidimensional intermolecular interactions in the solid state, desirable features for application in crystal engineering, and facilitate supramolecular assembly.³ Therefore, over the past decade intensive effort has been devoted to the synthesis of heterohelicenes with multihelicity.⁴ However, to the best of our knowledge, the incorporation of boron atoms into multihelical π -conjugated systems has not been established so far due to the lack of a suitable methodology and requirement of a multistep synthesis. Herein, we report a facile and scalable synthesis of double [5]helicenes possessing two boronate substructures at the ring junction (Scheme 1). The key to success is the combined use of Hart reaction⁵ and boron-assisted demethylative cyclization, which enable us to construct the helicene skeleton in two steps from commercially available compounds. Parent helicene **1a** shows excellent ambipolar conductivity, and derivative **1b** containing four *tert*-butyl groups exhibits efficient circularly polarized luminescence, suggesting potential applications in materials science.

The synthesis of **1a** and **1b** is summarized in Scheme 1. The Hart reaction between hexabromobenzene and *o*-anysylmagnesium bromide proceeded smoothly at 50 °C to afford 2,3,5,6-tetra(*o*-anysyl)-1,4-diiodobenzene **2a** in 21% yield upon

Scheme 1. Synthesis of Boron-Fused Double [5]Helicenes



iodination quenching. Lithium-halogen exchange in **2a** and subsequent trapping of the resulting aryllithium with boron tribromide gave the diborylated intermediate **3a**, which readily underwent boron-assisted demethylative cyclization at 40 °C to afford **1a** in 55% yield. The introduction of bulky *tert*-butyl groups did not interfere with these reactions: **1b** was prepared from hexabromobenzene in two steps, demonstrating the versatility of the strategy. Notably, **1a** and **1b** show substantial chemical and thermal stability: decomposition was not observed during silica gel column chromatography or heating at 200 °C in air.

The helical structure of **1a** was determined by X-ray crystallography (Figure 1a). The B–C and B–O bond lengths are 1.518–1.522 and 1.369–1.371 Å, respectively, indicating their single bond character. Furthermore, the C1–C2 and C4–C6 bond lengths (1.411(2) and 1.409(2) Å, respectively) are much shorter than that of the C2–C4 bond (1.477(2) Å). The strong bond alternation of the BOC₄ rings may account for the small nucleus-independent chemical shift (NICS(0)) value⁶ of 1.3 (Figure 1c). In contrast, the surrounding C₆ rings, including the distorted central benzene ring, show large negative

Received: February 15, 2016

Published: April 6, 2016

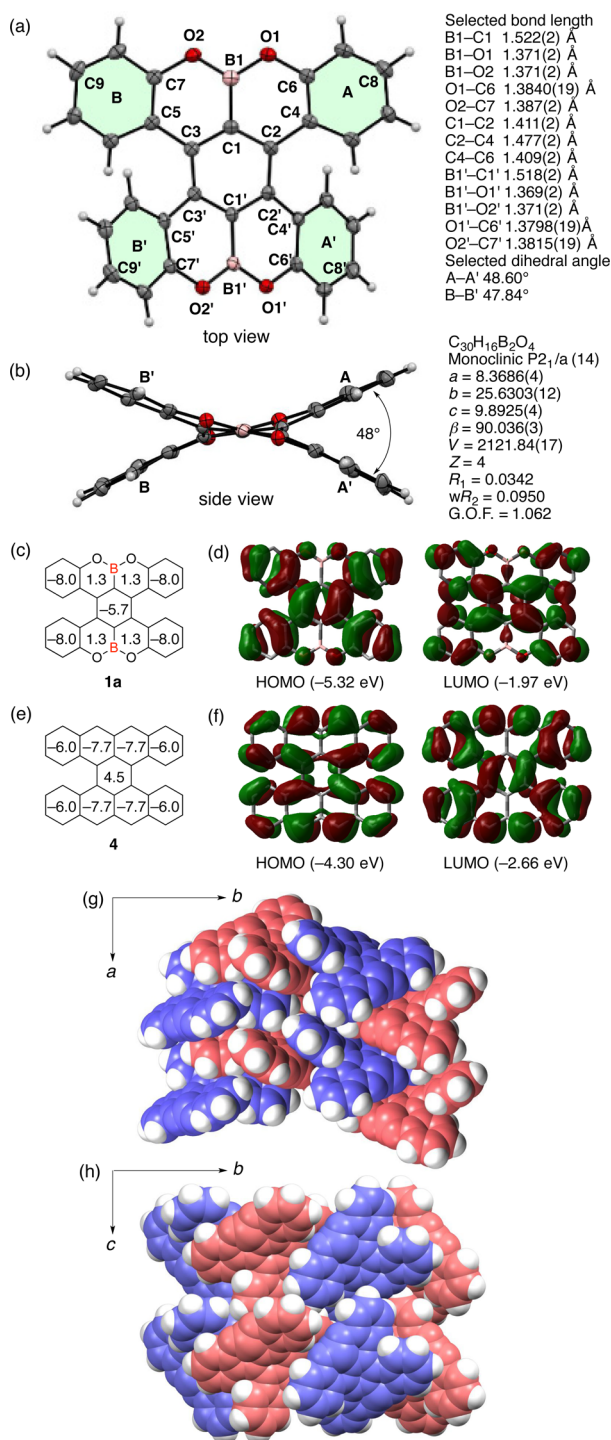


Figure 1. (a,b) ORTEP drawing and (g,h) packing structure of **1a** obtained by X-ray crystal analysis. Thermal ellipsoids are shown at 50% probability. (*P,P*)-isomer, blue; (*M,M*)-isomer, pink. NICS(0) values and the Kohn–Sham highest occupied molecular orbital (HOMO) and lowest unoccupied molecular orbital (LUMO) of **1a** (c,d) and tetrabenz[*a,f,j,j*,*o*]perylene (e,f) are also shown.

NICS(0) values. Notably, molecular orbital calculations indicate that the HOMO and LUMO are spread over the C_6 rings rather than the boron and oxygen atoms, accounting for the substantial stability of **1a** (Figure 1d). The NICS(0) values and HOMO and LUMO of carbon analogue **4**, tetrabenz[*a,f,j,j*,*o*]perylene,⁷ are shown in Figures 1e,f. In stark contrast,

the central C_6 ring shows a positive NICS(0) value, indicating substantial antiaromatic character. The dihedral angles between the planes of the terminal rings (A–A' and B–B') are comparable (48°) to that of the optimized structure of **4** (49°) from density functional theory (DFT) calculations.⁶ The unique 3D packing structure of the heterochiral crystal is shown in Figure 1g,h. The (*P,P*)- and (*M,M*)-isomers are arranged in an offset face-to-face stacking array along the *a*-axis with a π – π distance of 3.2–3.4 Å. In the heterochiral array, unilateral tetracenes do not contribute significantly to the π -stacking along the *a*-axis and thus interact with the adjacent heterochiral array along the *b*-axis to build the brickwork arrangement (Figure 1g).⁸ Moreover, both the tetracenes interact with the adjacent array along the *c*-axis to build the herringbone arrangement (Figure 1h). Such 3D π -stacking is ideal for application as a semiconducting material. The structure of derivative **1b** was also determined by X-ray crystallography.⁹ Due to the bulkiness of the *tert*-butyl groups and incorporation of the solvent used for recrystallization, efficient π -stacking was not observed. Notably, the introduction of *tert*-butyl groups does not substantially change the helical structure, but does interfere with the π -stacking.

Encouraged by the unique brickwork arrangement, we investigated the carrier-transport properties of **1a** by time of flight (TOF) measurements.⁹ Vacuum-deposition was conducted at 5.0×10^{-3} Pa to give a stable amorphous film (thickness: 3.6 μm) and then the transient photocurrent was measured under electric fields of 2.0 – 3.5×10^5 V cm^{-1} (Figure 2). Helicene **1a** showed balanced ambipolar conductivity ($\mu_h =$

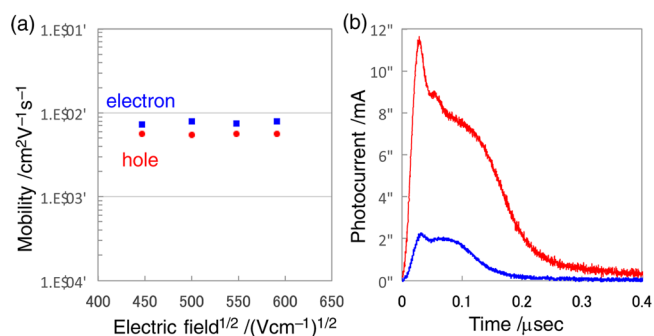


Figure 2. (a) Logarithmic mobilities of **1a** versus the square root of the electric field and (b) photocurrent profiles under an electric field of 3.5×10^5 V cm^{-1} for holes (red) and electrons (blue).

5.7×10^{-3} $\text{cm}^2 \text{V}^{-1} \text{s}^{-1}$, $\mu_e = 7.9 \times 10^{-3}$ $\text{cm}^2 \text{V}^{-1} \text{s}^{-1}$), superior to those of representative amorphous ambipolar materials, CBP ($\mu_h = 2 \times 10^{-3}$ $\text{cm}^2 \text{V}^{-1} \text{s}^{-1}$, $\mu_e = 3 \times 10^{-4}$ $\text{cm}^2 \text{V}^{-1} \text{s}^{-1}$)¹⁰ and mCP ($\mu_h = 3.2 \times 10^{-4}$ $\text{cm}^2 \text{V}^{-1} \text{s}^{-1}$, $\mu_e = 2.0 \times 10^{-4}$ $\text{cm}^2 \text{V}^{-1} \text{s}^{-1}$),¹¹ indicating its high potential for materials science applications.

To obtain deeper insight into the dynamic behavior of **1a** and **1b**, DFT calculations were conducted for the isomerization process (Figure 3).⁶ The isomerization barrier (ΔG^\ddagger) from chiral isomers ((*P,P*)- or (*M,M*)-**1a**) to the *meso* isomer ((*P,M*)-**1a**) was 23.0 kcal mol^{-1} (at 298.15 K), which is comparable to that of [*S*]helicene.¹² Notably, the *meso* isomer was less stable than the chiral isomers by 5.0 kcal mol^{-1} , which accounts for its nondetection during the preparation of **1a**. The isomerization barrier was substantially increased (31.8 kcal mol^{-1}) by introducing *tert*-butyl groups, which allowed us to separate (*P,P*)- and (*M,M*)-**1b** by chiral HPLC on a DAICEL

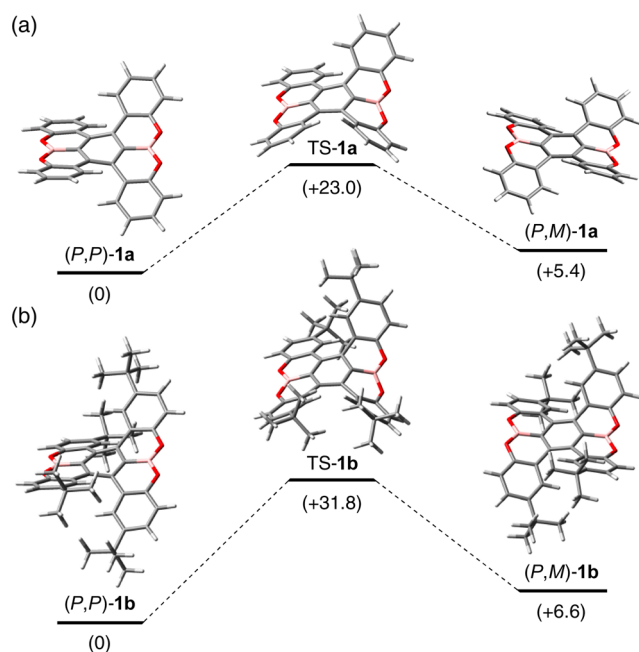


Figure 3. Isomerization process for (a) **1a** and (b) **1b** calculated at the B3LYP/6-31G(d) level. Relative Gibbs free energy (kcal mol^{-1}) is shown in parentheses.

CHIRALPAK IE-3 column (eluent: toluene). By using one of the chiral isomers, the isomerization barrier was determined as $29.0 \text{ kcal mol}^{-1}$,⁹ which agrees fairly well with that estimated by DFT calculation.

The photophysical properties of **1a** and **1b** in CH_2Cl_2 are summarized in Figure 4. As shown in Figure 4a,b, the UV–visible absorption and fluorescence spectra of **1b** are slightly red-shifted ($\lambda_{\text{ab}}, \lambda_{\text{em}} = 411, 436 \text{ nm}$) from those of **1a** ($\lambda_{\text{ab}}, \lambda_{\text{em}} = 405, 430 \text{ nm}$) due to hyperconjugation between the *tert*-butyl

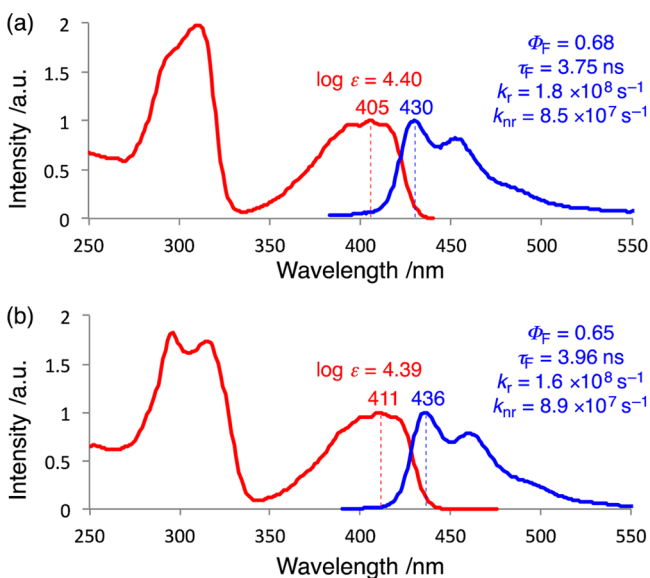


Figure 4. Normalized absorption (red) and fluorescence (blue) spectra of (a) **1a** and (b) **1b** (0.02 mM in CH_2Cl_2) with photophysical data. Abbreviations: ϵ , absorption coefficient at an absorption maximum; Φ_{F} , absolute PL quantum yield; τ_{F} , fluorescence lifetime measured at an emission maximum; k_{r} , radiative rate constant; k_{nr} , nonradiative rate constant.

groups and the π -system. These absorption and emission bands were assigned by time-dependent DFT (TD-DFT) calculations to HOMO–LUMO transitions.⁶ Commission Internationale de l’Eclairage coordinates of **1a** and **1b** are (0.15, 0.05) and (0.15, 0.08), which are very close to the color coordinates for pure blue, (0.15, 0.06), defined by Adobe RGB and suitable for organic light-emitting diodes. Notably, the absolute fluorescence quantum yields of **1a** and **1b** are 68% and 65%, respectively, which are record-setting values for double helicenes.³ The fluorescence lifetimes and radiative and nonradiative decay rate constants of **1a** and **1b** are almost identical, suggesting that the introduction of *tert*-butyl groups can suppress isomerization with negligible effects on the photophysical properties. Figure 5 shows the circular dichroism

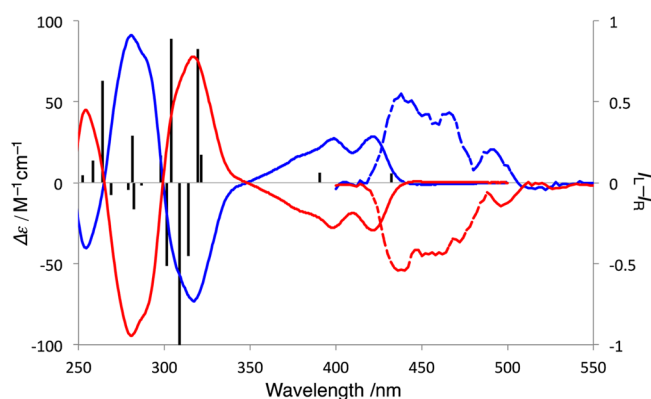


Figure 5. CD (solid line) and CPL (dotted line) spectra of (*P,P*)-**1b** (red) and (*M,M*)-**1b** (blue) (0.01 mM in CH_2Cl_2). The black lines show the CD spectrum for (*M,M*)-**1b** calculated by TD-DFT at the B3LYP/6-311+G(d,p) level.

(CD) spectra of **1b** in CH_2Cl_2 . The spectra of the two enantiomers appear as mirror images, and the absolute configuration of each enantiomer was determined by comparison with the CD spectra obtained by TD-DFT calculations. Notably, **1b** exhibits circularly polarized luminescence (CPL) activity. The CPL anisotropy factor (g_{lum}) was measured as 1.7×10^{-3} for both enantiomers, which is comparable to the values observed for other helicenes.^{2–4}

In summary, we developed a two-step protocol for the synthesis of boron-fused double [5]helicenes. The novel double helicenes show excellent ambipolar conductivity, deep blue fluorescence, and CPL activity, suggesting their potential as (opto)electronic materials. The simple and scalable protocol is promising for further extension of the π -system and introduction of various heteroatoms, which will provide functional materials with multihelicity.

■ ASSOCIATED CONTENT

Supporting Information

The Supporting Information is available free of charge on the ACS Publications Web site. The Supporting Information is available free of charge on the ACS Publications website at DOI: 10.1021/jacs.6b01674.

Synthesis, analytical data, NMR spectra, DFT studies, photophysical studies, X-ray crystallography data, TOF measurements (PDF)
Compound **1a** (CIF)
Compound **1b** (CIF)

AUTHOR INFORMATION

Corresponding Author

*hatake@kwansei.ac.jp

Notes

The authors declare no competing financial interest.

ACKNOWLEDGMENTS

This study was supported by a Grant-in-Aid for Scientific Research on Innovative Areas “ π -System Figuration: Control of Electron and Structural Dynamism for Innovative Functions” (15H01004), a Grant-in-Aid for Scientific Research (26288095) from the Ministry of Education, Culture, Sports, Science & Technology in Japan (MEXT). We thank Prof. Hikaru Takaya (Kyoto University) for his support for X-ray crystallography, Mr. Toshiaki Ikuta (JNC Petrochemical Corporation) for TOF measurement, Mr. Fumiya Miyamoto (Kwansei Gakuin University) for his experimental support, and Dr. Yasushi Honda (HPC Systems Inc.) for valuable discussions. The synchrotron X-ray diffraction measurements were performed at the BL40XU beamline in SPring-8 with the approval of JASRI (2014B1815, 2015A1320, 2015B0123). J. Kumar is grateful for Research Fellowships for Postdoctoral Researchers (PU14011) from the Japan Society for the Promotion of Science (JSPS).

REFERENCES

- (1) Recent reviews: (a) Shen, Y.; Chen, C.-F. *Chem. Rev.* **2012**, *112*, 1463. (b) Gingras, M. *Chem. Soc. Rev.* **2013**, *42*, 968. (c) Gingras, M.; Félix, G.; Peresutti, R. *Chem. Soc. Rev.* **2013**, *42*, 1007. (d) Gingras, M. *Chem. Soc. Rev.* **2013**, *42*, 1051. (e) Peng, Z.; Takenaka, N. *Chem. Rec.* **2013**, *13*, 28. (f) Yamaguchi, M.; Shigeno, M.; Saito, N.; Yamamoto, K. *Chem. Rec.* **2014**, *14*, 15. (g) Tanaka, K.; Kimura, Y.; Murayama, K. *Bull. Chem. Soc. Jpn.* **2015**, *88*, 375.
- (2) Recent examples (a) Pieters, G.; Gaucher, A.; Marque, S.; Maurel, F.; Lesot, P.; Prim, D. *J. Org. Chem.* **2010**, *75*, 2096. (b) Shinohara, K.; Sannohe, Y.; Kaieda, S.; Tanaka, K.; Osuga, H.; Tahara, H.; Xu, Y.; Kawase, T.; Bando, T.; Sugiyama, H. *J. Am. Chem. Soc.* **2010**, *132*, 3778. (c) Kaseyama, T.; Furumi, S.; Zhang, X.; Tanaka, K.; Takeuchi, M. *Angew. Chem., Int. Ed.* **2011**, *50*, 3684. (d) Nakano, K.; Oyama, H.; Nishimura, Y.; Nakasako, S.; Nozaki, K. *Angew. Chem., Int. Ed.* **2012**, *51*, 695. (e) Zadny, J.; Jancarik, A.; Andronova, A.; Samal, M.; Chocholousova, J. V.; Vacek, J.; Pohl, R.; Saman, D.; Cisarova, I.; Stara, I. G.; Sary, I. *Angew. Chem., Int. Ed.* **2012**, *51*, 5857. (f) Goto, K.; Yamaguchi, R.; Hiroto, S.; Ueno, H.; Kawai, T.; Shinokubo, H. *Angew. Chem., Int. Ed.* **2012**, *51*, 10333. (g) Hatakeyama, T.; Hashimoto, S.; Oba, T.; Nakamura, M. *J. Am. Chem. Soc.* **2012**, *134*, 19600. (h) Kaneko, E.; Matsumoto, Y.; Kamikawa, K. *Chem. - Eur. J.* **2013**, *19*, 11837. (i) Yavari, K.; Aillard, P.; Zhang, Y.; Nuter, F.; Retailleau, P.; Voituriez, A.; Marinetti, A. *Angew. Chem., Int. Ed.* **2014**, *53*, 861. (j) Gouin, J.; Bürgi, T.; Guéenne, L.; Lacour, J. *Org. Lett.* **2014**, *16*, 3800. (k) Gicquel, M.; Zhang, Y.; Aillard, P.; Retailleau, P.; Voituriez, A.; Marinetti, A. *Angew. Chem., Int. Ed.* **2015**, *54*, 5470. (l) Matsuno, T.; Koyama, Y.; Hiroto, S.; Kumar, J.; Kawai, T.; Shinokubo, H. *Chem. Commun.* **2015**, *51*, 4607. (m) Hirai, H.; Nakajima, K.; Nakatsuka, S.; Shiren, K.; Ni, J.; Nomura, S.; Ikuta, T.; Hatakeyama, T. *Angew. Chem., Int. Ed.* **2015**, *54*, 13581. (n) Hasan, M.; Pandey, A. D.; Khose, V. N.; Mirgane, N. A.; Karnik, A. V. *Eur. J. Org. Chem.* **2015**, *17*, 3702. (o) Shyam Sundar, M.; Bedekar, A. V. *Org. Lett.* **2015**, *17*, 5808. (p) Schickedanz, K.; Trageser, T.; Bolte, M.; Lerner, H.-W.; Wagner, M. *Chem. Commun.* **2015**, *51*, 15808. (q) Miyamoto, F.; Nakatsuka, S.; Yamada, K.; Nakayama, K.; Hatakeyama, T. *Org. Lett.* **2015**, *17*, 6158.
- (3) (a) Pena, D.; Cobas, A.; Perez, D.; Guitian, E.; Castedo, L. *Org. Lett.* **2003**, *5*, 1863. (b) Chen, T.-A.; Liu, R.-S. *Org. Lett.* **2011**, *13*, 4644. (c) Eversloh, C. L.; Liu, Z.; Müller, B.; Stangl, M.; Li, C.; Müllen, K. *Org. Lett.* **2011**, *13*, 5528. (d) Luo, J.; Xu, X.; Mao, R.; Miao, Q. *J. Am. Chem. Soc.* **2012**, *134*, 13796. (e) Xiao, S.; Kang, S. J.;

- Wu, Y.; Ahn, S.; Kim, J. B.; Loo, Y.-L.; Siegrist, T.; Steigerwald, M. L.; Li, H.; Nuckolls, C. *Chem. Sci.* **2013**, *4*, 2018. (f) Zhong, Y.; Kumar, B.; Oh, S.; Trinh, M. T.; Wu, Y.; Elbert, K.; Li, P.; Zhu, X.; Xiao, S.; Ng, F.; Steigerwald, M. L.; Nuckolls, C. *J. Am. Chem. Soc.* **2014**, *136*, 8122. (g) Kashihara, H.; Asada, T.; Kamikawa, K. *Chem. - Eur. J.* **2015**, *21*, 6523. (h) Ball, M.; Zhong, Y.; Wu, Y.; Schenck, C.; Ng, F.; Steigerwald, M.; Xiao, S.; Nuckolls, C. *Acc. Chem. Res.* **2015**, *48*, 267. (i) Fujikawa, T.; Segawa, Y.; Itami, K. *J. Am. Chem. Soc.* **2015**, *137*, 7763.
- (4) (a) Shiraishi, K.; Rajca, A.; Pink, M.; Rajca, S. *J. Am. Chem. Soc.* **2005**, *127*, 9312. (b) Wang, Z.; Shi, J.; Wang, J.; Li, C.; Tian, X.; Cheng, Y.; Wang, H. *Org. Lett.* **2010**, *12*, 456. (c) Liu, X.; Yu, P.; Xu, L.; Yang, J.; Shi, J.; Wang, Z.; Cheng, Y.; Wang, H. *J. Org. Chem.* **2013**, *78*, 6316. (d) Hashimoto, S.; Nakatsuka, S.; Nakamura, M.; Hatakeyama, T. *Angew. Chem., Int. Ed.* **2014**, *53*, 14074. (e) Nakamura, K.; Furumi, S.; Takeuchi, M.; Shibuya, T.; Tanaka, K. *J. Am. Chem. Soc.* **2014**, *136*, 5555. (e) Sakamaki, D.; Kumano, D.; Yashima, E.; Seki, S. *Angew. Chem., Int. Ed.* **2015**, *54*, 5404.
- (5) Harada, K.; Hart, H.; Du, C. J. F. *J. Org. Chem.* **1985**, *50*, 5524.
- (6) DFT calculations were performed using the B3LYP hybrid functional with the 6-31G(d) basis set implemented in the Gaussian 09 program. NICS and TD-DFT calculations were conducted with the 6-311+G(d,p) basis set. See the [Supporting Information](#) for details.
- (7) Liu, J.; Ravat, P.; Wagner, M.; Baumgarten, M.; Feng, X.; Müllen, K. *Angew. Chem., Int. Ed.* **2015**, *54*, 12442.
- (8) Shan, L.; Liu, D.; Li, H.; Xu, X.; Shan, B.; Xu, J.-B.; Miao, Q. *Adv. Mater.* **2015**, *27*, 3418.
- (9) See the [Supporting Information](#) for details.
- (10) Matsushima, H.; Naka, S.; Okada, H.; Onnagawa, H. *Curr. Appl. Phys.* **2005**, *5*, 305.
- (11) Jou, J.-H.; Wang, W.-B.; Chen, S.-Z.; Shyue, J.-J.; Hsu, M.-F.; Lin, C.-W.; Shen, S.-M.; Wang, C.-J.; Liu, C.-P.; Chen, C.-T.; Wu, M.-F.; Liu, S.-W. *J. Mater. Chem.* **2010**, *20*, 8411.
- (12) Goediche, Ch.; Stegemeyer, H. *Tetrahedron Lett.* **1970**, *12*, 937.